ISSN 0023-1584, Kinetics and Catalysis, 2009, Vol. 50, No. 2, pp. 228–234. © Pleiades Publishing, Ltd., 2009.
Published in Russian in Kinetika i Kataliz, 2009, Vol. 50, No. 2, pp. 242–248.

The Effect of Spinel Type Support $FeAlO_3$, $ZnAl_2O_4$, $CrAl_3O_6$ on Physicochemical Properties of Cu, Ag, Au, Ru Supported Catalysts for Methanol Synthesis[1]

T. P. Maniecki, P. Mierczyński, W. Maniukiewicz, D. Gebauer, and W. K. Jozwiak

Technical University of Łódź, Poland

Institute of General and Ecological Chemistry, Żeromskiego 116, 90-924 Łódź, Poland

e-mail: tmanieck@p.lodz.pl

Received October 16, 2007

Abstract—The comparative study of the role of binary oxide support on catalyst physico-chemical properties and performance in methanol synthesis were undertaken and the spinel like type structures ($ZnAl_2O_4$, $FeAlO_3$, $CrAl_3O_6$) were prepared and used as the supports for 5% metal (Cu, Ag, Au, Ru) dispersed catalysts. The monometallic 5% Cu/support and bimetallic 1% Au (or 1% Ru)–5% Cu/support (Al_2O_3, $ZnAl_2O_4$, $FeAlO_3$, $CrAl_3O_6$) catalysts were investigated by BET, XRD and TPR methods. Activity tests in methanol synthesis of CO and CO_2 mixture hydrogenation were carried out. The order of Cu/support catalysts activity in methanol synthesis: $CrAl_3O_6 > FeAlO_3 > ZnAl_2O_4$ is conditioned by their reducibility in hydrogen at low temperature. Gold appeared more efficient than ruthenium in promotion of Cu/support catalysts.

DOI: 10.1134/S0023158409020128

1. INTRODUCTION

Industrial methanol is produced from natural gas or coal via syngas, which has been developed by ICI, Lurgi, Topsone and MTC companies in the last century [1]. Methanol synthesis involving the hydrogenation of a mixture of carbon monoxide and dioxide occurs according to the following equations:

$$\begin{gathered} CO + 2H_2 \longrightarrow CH_3OH, \\ \Delta H^0_{298} = -90.6 \text{ kJ/mol}, \end{gathered} \quad (I)$$

$$\begin{gathered} CO_2 + 3H_2 \longrightarrow CH_3OH + H_2O, \\ \Delta H^0_{298} = -49.5 \text{ kJ/mol}. \end{gathered} \quad (II)$$

Both reactions are similar not only because they refer to the same product—methanol but they are mutually correlated by the reverse of water gas shift reaction (WGS) being the resultant of subtraction between Eqs. (II) and (I) being expressed by following equation:

$$\begin{gathered} CO_2 + H_2 \longrightarrow CO + H_2O, \\ \Delta H^0_{298} = 41.1 \text{ kJ/mol}. \end{gathered} \quad (III)$$

According to LeChatelier's rule the comparison of enthalpy effects confirm that low temperature range of reaction would favor moderately exothermic methanol synthesis reactions (I) and (II) in contrast with the resultant of slightly endothermic effects of reverse WGS reaction (III). Thus, in syngas mixture containing carbon dioxide or water components the accompanying and unavoidable reactions (II) and (III) are involved in main methanol synthesis reaction (I). Methanol is synthesized from CO, CO_2 and H_2 over Cu/ZnO based catalysts due to synthesis from CO_2 began at a temperature lower than that from CO and proceeded at a faster rate [2]. However addition of a small amount of CO_2 (2–5%) to syngas can promote methanol yield remarkably [3]. At 300°C and 5.0 MPa, the degree of CO conversion is about 20% [4]. Methanol synthesis usually takes place in the temperature range 280–300°C on $Cu–ZnO–Al_2O_3$ catalyst in ICI process [5].

Recently, the process of methanol synthesis from carbon dioxide and hydrogen has been extensively studied [6–8] and methanol obtained by CO_2 hydrogenation appeared more expensive than that obtained from CO and 2–5% CO_2 mixture in reaction conditions: 0.1–10 MPa and 225–285°C [9–11].

In numerous papers referring to copper catalysts one can find many single metal oxide supports: such as Al_2O_3 [12], Cr_2O_3 [13], TiO_2 [12], ZnO [13, 14], ZrO_2 [15, 16] and their combination [13, 14] used in methanol synthesis. For example copper supported on binary oxide $3ZnO \cdot ZrO_2$ appeared more active than silver or gold catalysts [17]. The selectivity to methanol from 11 to 43% was observed for zirconia modified Cu/SiO_2 catalyst [18]. The considerable improvement of methanol selectivity and activity was reported depending on $Cu/\gamma\text{-}Al_2O_3(ZrO_2)$ catalyst preparation method (co-precipitation, impregnation, leaching, and deposition—precipitation) [13–18].

[1] The article is published in the original.

Table 1. Specific surface area of supports and metal supported catalysts

Support/T_{calc}, °C	Surface area, m^2/g	5% Me/$FeAlO_3$, 400°C	Surface area, m^2/g
Al_2O_3 (400)	237	Cu/$FeAlO_3$	144
$ZnAl_2O_4$ (600)	87	Ag/$FeAlO_3$	150
$FeAlO_3$ (500)	143	Au/$FeAlO_3$	112
$CrAl_3O_6$ (700)	82	Ru/$FeAlO_3$	143

The comparative study of the role of binary oxide support on catalyst performance in methanol synthesis were undertaken in this work. The spinel like type structures ($ZnAl_2O_4$, $FeAlO_3$, $CrAl_3O_6$) were prepared and used as the supports for 5% metal (Cu, Ag, Au, Ru) dispersed catalysts. The structure and catalytic performance of supports and metal supported catalysts were investigated by BET, XRD and TPR methods. Activity tests in methanol synthesis of CO and CO_2 mixture hydrogenation were carried out.

2. EXPERIMENTAL

2.1. Preparation of Catalysts

Catalysts were prepared by wet aqueous impregnation method. To prepare the support precursors, nitrates of Al, Cr, Fe and zinc acetate were used. The ammonia co-precipitated binary mixtures of aluminium hydroxide with the appropriate zinc, iron or chromium hydroxides were dried and calcined 3 h in air at 600, 500 and 700°C. The composition of binary oxides: $ZnAl_2O_4$, $FeAlO_3$, and $CrAl_3O_6$ is reflected by molar ratio: Al/Zn = 2, Al/Fe = 1 and Al/Cr = 3, respectively. Metal phase 5% Me (Cu, Ag, Au, Ru) was dispersed on appropriate support by impregnation method and then the catalysts were dried and finally calcined 4 h in air at 400°C.

2.2. Methods of Characterization

Catalysts and supports were characterised by X-ray diffraction, BET surface area measurements and temperature programmed reduction (TPR-H_2). Phase composition was analysed by XRD diffraction method using PAN analytical X'Pert MPD diffractometer (in 2θ range (20°–80°)). The specific surface area and porosity for catalysts and supports were determined with automatic sorptometer Sorptomatic 1900. Samples were carefully evacuated at 250°C and after that low temperature BET nitrogen adsorption-desorption were carried out. The TPR-H_2 measurements were carried out in automatic TPR system AMI-1 in temperature range 25–900°C with the linear heating rate 10 K/min. Samples (about 0.1 g) were reduced in hydrogen stream (5% H_2–95% Ar) with volume velocity 40 cm^3 per minute. Hydrogen consumption was monitored by a thermal conductivity detector (TCD).

2.3. Catalytic Activity Test

Hydrogenation tests of CO/CO_2 mixture were carried out using a flow quartz reactor in the temperature range 200–380°C combined on line with GC detector. Preliminary all catalysts were reduced for 2 h in H_2 flow at 300°C and atmospheric pressure. Before syngas exposure catalysts were cooled to the reaction temperature and then hydrogen stream was switch to atmospheric pressure syngas mixture with molar ratio CO : CO_2 : H_2 being 2 : 1 : 4 and volume velocity 56 cm^3/min. The steady-state activity measurements were taken after at least 12 h on the stream. The analysis of the reaction products were carried out by on line a gas chromatograph equipped with FID detector and column containing 10% Carbowax on Chromosorb W-aw.

3. RESULTS AND DISCUSSION

3.1. Surface Area and Porosity

Results of specific surface area measurements for supports (Al_2O_3, $ZnAl_2O_4$, $FeAlO_3$, $CrAl_3O_6$) and metal (Cu, Ag, Au, Ru)/$FeAlO_3$ catalysts are presented in Table 1.

One can see that binary spinel oxides are characterised by considerable lower specific surface area about 40–70% than alumina itself. In the case of $FeAlO_3$ spinel metal/support catalysts the introduction of metallic phase 5% Me (Cu, Ag, Ru) practically does not change the surface area being about 150 m^2/g except for Au/$FeAlO_3$ catalyst where more than 20% decrease was attributed to the action of strongly acidic gold nitrate solution during support impregnation.

The results of pore size distribution measurements for binary supports $ZnAl_2O_4$, $FeAlO_3$, $CrAl_3O_6$, and Al_2O_3 are presented in Fig. 1. All supports have the pore radius in the range 18–85 Å. Although the pore size distribution in all cases is similar to the Al_2O_3 porosity the relative changes of pore volume and radius are attributed to the different degree of crystallinity acquired during binary oxides calcination.

3.2. Phase Composition

The XRD patterns of supports $ZnAl_2O_4$, $FeAlO_3$, and $CrAl_3O_6$ are presented in Fig. 2a. Highly amorphous and disordered character was demonstrated in the case of alumina itself whereas the presence of more or less crystalline spinel structures was confirmed for

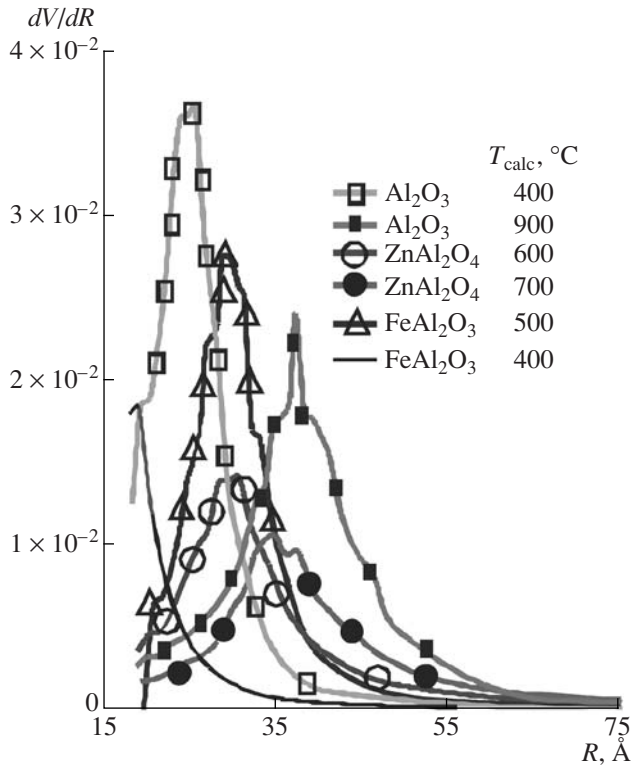

Fig. 1. The pore size distribution of Al_2O_3, $ZnAl_2O_4$, $FeAlO_3$, $CrAl_3O_6$ supports.

binary oxides [19–22]. In the case of $FeAlO_3$ spinel the main spinel structure was accompanied by traces of highly amorphous disordered structures of alumina γ-Al_2O_3 and hematite Fe_2O_3. Also dominant crystalline spinel phase of $CrAl_3O_6$ is accompanied by chromia α-Cr_2O_3. In the case of XRD pattern of $ZnAl_2O_4$ sample the characteristic reflexes of only zinc- aluminium spinel structure were detected.

The XRD patterns for supported metals 5% Me (Cu, Ag, Au, Ru) dispersed on $FeAlO_3$ spinel support after catalysts calcination at 400°C are presented in Fig. 2b. The lack of detectable crystal metal oxide phases of Cu, Ag, Ru indirectly confirms high degree of metal dispersion on $FeAlO_3$ surface (crystallite size < 5 nm). Only in the case of 5% Au/$FeAlO_3$ catalyst the presence of metallic gold phase is evident as a result of reductive decomposition of Au_2O_3 phase during catalyst calcination.

Table 2. Reduction degree for $ZnAl_2O_4$ supported catalysts

Catalyst	Degree of reduction, %
5% Cu/$ZnAl_2O_4$	64
5% Ag/$ZnAl_2O_4$	32
5% Au/$ZnAl_2O_4$	0
5% Ru/$ZnAl_2O_4$	100

3.3. Temperature Programmed Reduction

The TPR profiles of 5% Me/support catalysts (metal—Cu, Ag, Au, Ru, support—Al_2O_3, $ZnAl_2O_4$, $FeAlO_3$, $CrAl_3O_6$) after their calcination 4 h in air at 400°C are presented in Figs. 3a–3d, respectively.

The TPR profiles for 5% Me (Au, Ag, Cu, Ru)/Al_2O_3 catalysts are presented in Fig. 3a. Reductive effects in low temperature range 100–300°C are only visible for copper and ruthenium supported catalysts and they can be assigned to hydrogen reduction of appropriate metal oxides CuO and RuO_2 to metallic phase ($CuO + H_2 \longrightarrow Cu + H_2O$ and $RuO_2 + 2H_2 \longrightarrow Ru + 2H_2O$). The obtained results are in good agreement with the literature data [23–25]. The relatively small reduction effect observed for 5% Cu/Al_2O_3 catalyst can be explained by partial oxidation of copper during calcination step. Additionally the formation of irreducible spinel structure can not be neglected [26]. The absence of reductive effects for 5% Au/Al_2O_3 and 5% Ag/Al_2O_3 catalysts confirms the instability of Au_2O_3 and Ag_2O oxide phases on alumina surface during catalyst calcination in air at 400°C.

The similar interpretation can be deduced for TPR profiles recorded for 5% Me/$ZnAl_2O_4$ catalysts which are presented in Fig. 3b. Zinc aluminate spinel shows only slight reduction effects in temperature range 600–900°C which seems to indicate the formation of oxygen vacancies ($O^{2-} + H_2 \longrightarrow V_O + H_2O$). The $ZnAl_2O_4$ spinel surface can stabilize dispersed CuO and RuO_2 crystallites but all of Au_2O_3 oxide and most of Ag_2O oxide phases undergo the reductive decomposition to metallic phases during catalyst calcination in air at 400°C. The calculated degrees of metal oxide reduction in 5% Me/$ZnAl_2O_4$ catalysts are gathered in Table 2.

The low reduction degree for 5% Ag/$ZnAl_2O_4$ catalyst being about 32% indicates that only small fraction of silver oxidic form can survive the calcination step on support surface whereas most of Ag_2O crystallite phase decomposes to metallic Ag and evolves gaseous oxygen. In the case of 5% Cu/$ZnAl_2O_4$ catalyst the reduction degree was about 64% and this value seems to suggest that considerable part of supported copper instead of being oxidized to CuO was rather oxidized to Cu_2O. This effect seems to indicate that zinc aluminate surface can stabilize supported copper as Cu^+ ions. As expected the presence of both gold metallic and ruthenium dioxide after calcination is confirmed by the estimated values of reduction degrees: zero for 5% Au/$ZnAl_2O_4$ and 100% for 5% Ru/$ZnAl_2O_4$ catalysts.

Comparison of TPR profiles recorded for Al_2O_3 and $ZnAl_2O_4$ supported metal catalysts shows rather similar behaviour of dispersed oxide phases and rather small relative differences in reduction temperature are attributed to weak metal oxide—support interactions known as SIMOS effects.

TPR profile obtained for support $FeAlO_3$ and 5% Me (Cu, Ag, Au, Ru)/$FeAlO_3$ catalysts are presented in

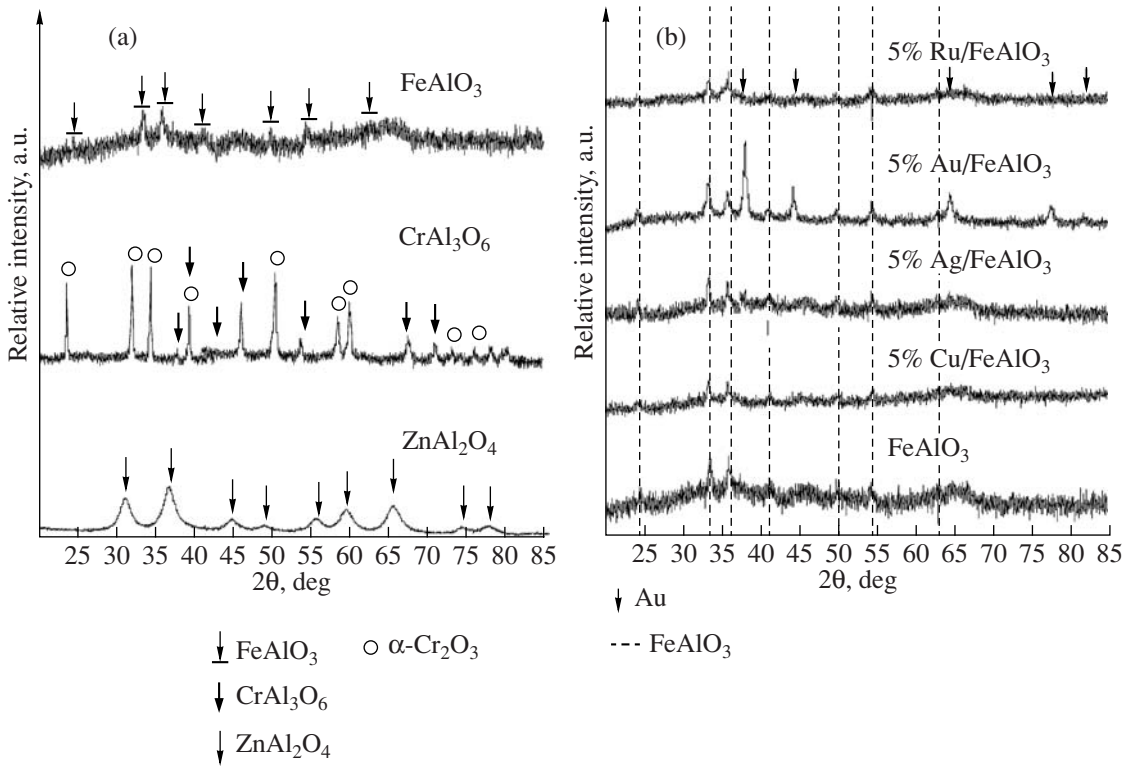

Fig. 2. XRD patterns for (a) Binary oxides $ZnAl_2O_4$, $FeAlO_3$, $CrAl_3O_6$, (b) Supported 5% Me (Cu, Ag, Au, Ru)/$FeAlO_3$ catalysts after calcination in air at 400°C.

Fig. 3c. Three reduction effects located at about 430, 720 and 890°C are observed for binary iron-aluminium oxide alone. These peaks can represent the reduction paths of oxidic forms of both iron and binary Fe–Al spinels structures and they can be described by two following schemes:

$$Fe_2O_3 \longrightarrow Fe_3O_4 \longrightarrow Fe \text{ and/or}$$
$$FeAlO_3 \longrightarrow Fe_2AlO_4 \longrightarrow FeAl_2O_4 \longrightarrow Fe \text{ [29].}$$

The first path refers to iron (III) oxide reduction: hematite > magnetite > metallic iron. Different mechanism of binary Fe-Al spinel reduction leads to final product—metallic iron and iron(II) aluminate $FeAl_2O_4$ hardly reducible in temperature range up to 900°C in 5% H_2–95% Ar stream. The overall reduction degree for binary support $FeAlO_3$ was rather low being about 37% (Table 3).

TPR runs for 5% Me(Cu, Ag, Ru)/$FeAlO_3$ catalysts shift considerably the reduction toward low temperature and these effects are assigned to the reduction of silver oxide/ferrate and CuO and RuO_2 phases, respectively. In the case of 5% Cu/$FeAlO_3$ and 5% Ru/$FeAlO_3$ catalysts the first stage of reduction $Fe_2O_3 \longrightarrow Fe_3O_4$ seems to be promoted by spillover of hydrogen atoms originating from H_2 dissociation taking place on already formed Cu or Ru metallic phases. The TPR profile of 5% Au/$FeAlO_3$ catalyst shows generally similar behaviour as support $FeAlO_3$ alone.

TPR profiles for 5% Me (Cu, Ag, Au, Ru)/$CrAl_3O_6$ catalysts are presented in the Fig. 3d. The profile for $CrAl_3O_6$ support itself exhibits one wide reduction effect in the temperature range 300–450°C and it was attributed to reduction of chromium oxidic forms CrO_x ($1.5 < x < 3$) formed during calcination step. At relatively low temperature of oxidation considerable amount of superficial Cr^{3+} ions can be oxidized to chromate like ions CrO_4^{2-} [27] and this is also the case of $CrAl_3O_6$ binary oxide. During hydrogen reduction the reverse process takes place ($CrO_x + xH_2 \longrightarrow 1/2\alpha\text{-}Cr_2O_3 + xH_2O$). In the case of efficient removal of water even reduction to Cr(II)O species can be anticipated [28].

Two reduction effects are reported for 5% Au/$CrAl_3O_6$ catalyst. First peak is assigned to the

Table 3. Reduction degree for $FeAlO_3$ supported catalysts

Support/Catalyst	Degree of reduction, %
$FeAlO_3$	37
5% Au/$FeAlO_3$	66
5% Ag/$FeAlO_3$	38
5% Ru/$FeAlO_3$	58
5% Cu/$FeAlO_3$	44

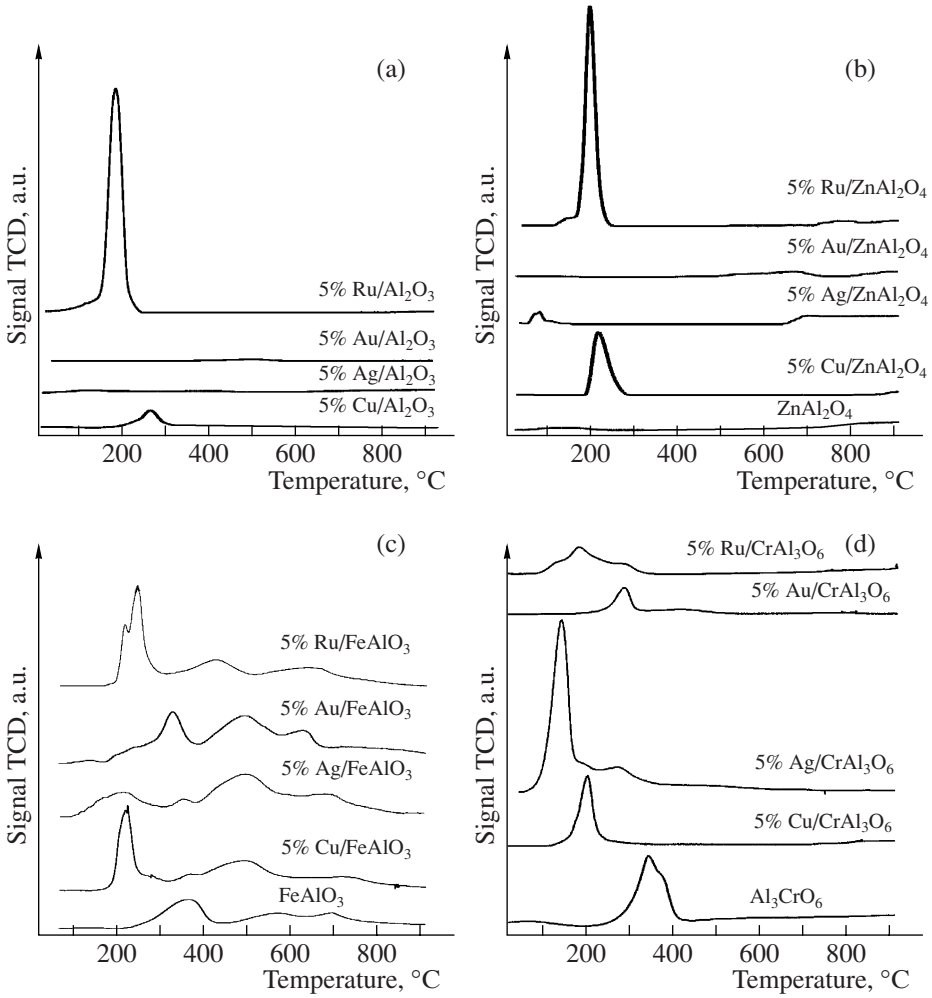

Fig. 3. TPR profiles (a) Me/Al_2O_3 catalysts, (b) $Me / ZnAl_2O_4$ catalysts, (c) $Me/CrAl_3O_6$ catalysts, (d) $Me/FeAlO_3$ catalysts.

reduction of superficial Cr^{6+} oxide form, shifted to lower temperature by about 50°C by promoting effect of metallic gold and second one can be attributed to the reduction of highly dispersed chromium(VI) oxide species strongly interacting with support surface.

TPR reduction profile for 5% $Ag/CrAl_3O_6$ catalyst is composed of three unresolved peaks. The first two effects at about 150 and 220°C probably originates from silver chromate forms differently interacting with the support ($Ag_2CrO_4 + 0.5H_2 \longrightarrow Ag + AgCrO_2 + 1/2\alpha\text{-}Cr_2O_3 + 0.5H_2O$). The last reduction peak can be attributed to the reduction of Cr^{6+} oxide species originating from support $CrAl_3O_6$.

Single and rather a symmetrical reduction peak is observed for 5% $Cu/CrAl_3O_6$ catalyst with a maximum of hydrogen consumption located at 190°C and it can be assigned to the reduction of dispersed CuO phase weakly interacting with support $CrAl_3O_6$.

The reduction profile for 5% $Ru/CrAl_3O_6$ catalyst consist of three partially resolved peaks which can be assigned to both, RuO_2 and RuO_2–CrO_3 surface species, less or more involved in SIMOS type interactions with support $CrAl_3O_6$.

4. ACTIVITY TESTS

The methanol synthesis tests were carried out on monometallic 5% Cu/support and bimetallic 1% Au (or 1% Ru)–5% Cu/support ($FeAlO_3$, $ZnAl_2O_4$, $CrAl_3O_6$) catalysts and the temperature characteristics of catalytic activity expressed in $\mu mol_{CH_3OH}\ g_{Cat}^{-1}\ h^{-1}$ are presented in Fig. 4. The methanol yield maximum is located in temperature range 240–280°C. Further increase of reaction temperature to 280°C leads to the significant fall of catalyst activity. The examined binary supports alone appeared totally inactive in methanol formation. The results received for monometallic copper supported catalysts show significant role of support reducibility on methanol yield. One can anticipate that catalyst activity increases together with its higher reducibility and the donor-acceptor ability for oxygen atoms. The decreasing order of 5% Cu/support was as

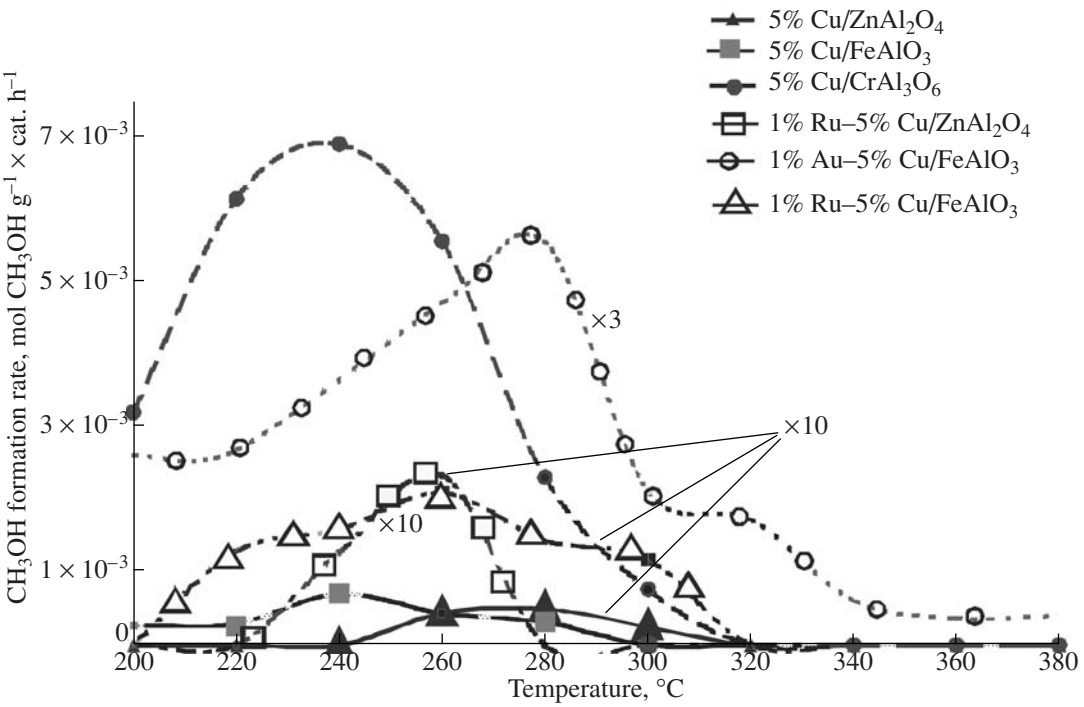

Fig. 4. Methanol formation rate as a function of reaction temperature for metal and bimetal supported catalysts.

follow: $CrAl_3O_6$ > $FeAlO_3$ > $ZnAl_2O_4$. Activity in methanol synthesis in similar condition was carried out in work [30]. Authors claims comparable activity.

Ruthenium added to mono-metallic Cu/support system promotes hydrogen dissociation on catalysts surface. On the other hand, one can anticipate that atomic hydrogen can reduce Cu^+ superficial active sites concentration. This fact seems to confirm lower activity of ruthenium doped catalyst in comparison to gold promoted catalysts. Gold addition increases significantly the amount of adsorbed carbon oxide on the catalyst surface, what can increase catalyst activity.

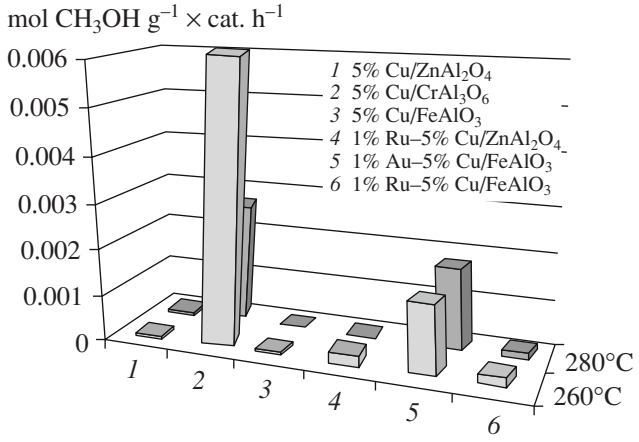

Fig. 5. The activity of mono and bimetallic catalysts in methanol synthesis at 260 and 280°C.

The comparison of methanol yield formation on different catalysts at temperatures 260 and 280°C is presented in Fig. 5. The methanol formation rate is in the range 5×10^{-5}–7×10^{-3} μmol_{CH_3OH} g_{Cat}^{-1} h^{-1} and it can be described by following order: 5% $Cu/CrAl_3O_6$ > 1% Au–5% $Cu/FeAlO_3$ > 1% Ru–5% $Cu/FeAlO_3$ > 1% Ru–5% $Cu/ZnAl_2O_4$ > 5% $Cu/FeAlO_3$ ≈ 5% $Cu/ZnAl_2O_4$.

5. CONCLUSIONS

• Specific surface area of meso-porous binary oxides: $ZnAl_2O_4$, $FeAlO_3$, and $CrAl_3O_6$ although is 40–70% lower than that characteristic of Al_2O_3 alone but many times higher than surface of the second individual crystalline oxide.

• The presence of spinel like crystalline structure for $FeAlO_3$, $ZnAl_2O_4$, $CrAl_3O_6$ was experimentally confirmed by XRD method.

• The reducibility of semireducible binary oxides $FeAlO_3$ and $CrAl_3O_6$ increases with the addition of active metals (Cu, Ru, and Au). The presence of chromate like oxides Ag_2CrO_4 and $CuCrO_4$ were anticipated on the bases of TPR data.

• The order of Cu/support catalysts activity in methanol synthesis: $CrAl_3O_6$ > $FeAlO_3$ > $ZnAl_2O_4$ seems to be conditioned by their low temperature reducibility in hydrogen.

• The gold addition is more efficient than ruthenium in promotion of Cu/support catalysts in methanol synthesis.

ACKNOWLEDGMENTS

The partial financial support of this work by the Polish Scientific Research Council supports (grant no. 1357/T09/2005/29) is gratefully acknowledged.

REFERENCES

1. Chinchen, G.C., Mansfield, K., and Spencer, M.S., *Chem.-Tech.*, 1990, no. 11, p. 5692.
2. Fujita, Sh., Usui, M., Ito, H., and Takezawa, N., *J. Catal.*, 1995, vol. 157, p. 403.
3. Sun, Q., Li, Ch., Pan, W., Zhu, Q., and Deng, J., *Appl. Catal., A*, 1998, vol. 171, p. 301.
4. Marchionna, M., Lami, M., and Galleti, A., *Chem.-Tech.*,1997, no. 4.
5. US Patent 1010871, 1966.
6. Haaggin, J., *Chem. Eng. News*, 1994, vol. 72, p. 29.
7. Hirano, M., Akano, T., Imai, T., and Kuroda, K., *Stud. Surf. Sci. Catal.*, 1998, vol. 114, p. 545.
8. Sloczynski, J., Grabowski, R., Kozlowska, A., Lachowska, M., and Skrzypek, J., *Stud. Surf. Sci. Catal.*, 2004, vol. 153, p. 161.
9. Breen, J.P. and Ross, J.R.H., *Catal. Today*, 1991, vol. 51, p. 521.
10. Velu, S., Suzuki, K., Okazaki, M., Kapoor, M.P., Osaki, T., and Ohashi, F., *J. Catal.*, 2000, vol. 194, p. 373.
11. De Wild, P.J. and Verhaak, M.J.F.M., *Catal. Today*, 2000, vol. 60, p. 3.
12. Bando, K.K., Sayama, K., Kusama, H., Okabe, K., and Arakowa, H., *Appl. Catal., A*, 1997, vol. 165, p. 391.
13. Ma, L., Tran, T., and Wainwright, M.S., *Top. Catal.*, 2003, vol. 22, p. 295.
14. Saito, M., Fujitani, T., Takeuchi, M., and Watanabe, T., *Appl. Catal., A*, 1996, vol. 138, p. 311.
15. Jung, K.D. and Bell, A.T., *J. Catal.*, 2000, vol. 193, p. 207.
16. Liu, J., Shi, J., He, D., Zhang, Q., Wu, X., Liang, Y., and Zhu, Q., *Appl. Catal., A*, 2001, vol. 218, p. 113.
17. Slomczynski, J., Grabowski, R., Kozlowska, A., Olszewski, P., Stoch, J., Skrzypek, J., and Lachowska, M., *Appl. Catal., A*, 2004, vol. 278, p. 11.
18. Fisher, I.A. and Bell, A.T., *J. Catal.*, 1997, vol. 172, p. 222.
19. Yanga, Ch., Chena, S., and Cheng, S., *Powder Technol.*, 2004, vol. 148, p. 3.
20. Li, Z., Zhang, Sh., and Lee, W.E., *J. Eur. Ceram. Soc.*, 2007, vol. 27, p. 3407.
21. Manetski, T.P., Bavolak, K., Gebauer, D., and Mierchinski, P., *Kinet. Katal.* (in press).
22. Nagai, T., Hamane, D., Sujatha Devi, P., Miyajima, N., Yagi, T., Yamanaka, T., and Fujino, K., *J. Phys. Chem. B*, 2005, vol. 109, p. 18226.
23. Kim, S.-K., Kim, K.-H., and Ihm, S.-K., *Chemosphere*, 2007, vol. 68, p. 287.
24. Siva Sankar Reddy, P., Pasha, N., Chalapathi Rao, M.G.V., Lingaiah, N., Suryanarayana, I., and Sai Prasad, P.S., *Catal. Commun.*, 2007, vol. 8, p. 1406.
25. Wen, H., Hwang, Ch., and Chang, H., *Appl. Catal., A*, 1997, vol. 162, p. 71.
26. Yahiro, H., Nakaya, K., Yamamoto, T., Saiki, K., and Yamaura, H., *Catal. Commun.*, 2006, vol. 7, p. 228.
27. Manetski, T.P., Bavolak, K., Gebauer, D., Mirchinski, P., and Yuzvyak, V.K., *Kinet. Katal.*, 2009, vol. 50, no. 1, p. 149 [*Kinet. Catal.* (Engl. Transl.), vol. 50, no. 1, p. 138].
28. Jóźwiak, W.K., Ignaczak, W., Dominiak, D., and Maniecki, T.P., *Appl. Catal., A*, 2004, vol. 258, p. 33.
29. Maniecki, T.P., Mierczyński, P., Maniukiewicz, D., Gebauer, D., Bawolak, K., and Jóźwiak, W.K., *Pol. J. Chem.*, (in press).
30. Abu-Zied, B.M., *Appl. Catal., A*, 2000, vol. 198, p. 139.